university of groningen / faculty of science and engineering

Investigating Chromatic Confocal Imaging

Author:
Gideon WIERSMA
(s4979796)

Supervisor:
prof. dr. Steven HOEKSTRA
Second examiner:
dr. Steven JONES
Daily supervisor:
ir. George SCHUT

Bachelor's Thesis
To fulfill the requirements for the degree of
Bachelor of Science in Physics
at the University of Groningen

July 2, 2025

Contents

Abstract

Schut Geometrical Metrology specializes in 3D coordinate measuring machines. To expand Schut's capabilities, this thesis investigates a novel technique called chromatic confocal imaging. In this technique, a small part of a measurement sample is imaged onto a pinhole. Due to chromatic aberrations, only a distance dependent wavelength is in focus at the pinhole. Therefore, the pinhole will isolate the in-focus light. By determining the correlation between the distance and the wavelength of the in focus light, the distance can be determined.

As a first prototype, a simplified version of the technique will be developed. The full technique involves also filtering the light coming onto the measurement sample but this prototype only filters the light coming off the sample.

This prototype will be suggested and tested simulation-wise. This study will investigate what configuration (pinhole size, aperture size, etc.) maximizes measurement accuracy. The simplified version assumes a measurement sample with only a small illuminated area. It will therefore be investigated how the size of this area influences the measurement accuracy.

This study focuses on two aspects of the set-up: the diameter of the aperture that is placed before the first lens and diameter of the pinhole that filters the light. It is found that, with the applied simplifications, an aperture diameter of 25 mm maximizes measurement accuracy. Furthermore, it is found that the pinhole diameter is inversely proportional to measurement accuracy but also inversely proportional signal strength of the detector. Therefore two prototypes are suggested: one that prioritizes signal strength and another that maximizes measurement accuracy. The pinholes diameter of these prototypes are 0.2 mm and 0.02 mm respectively.

Acknowledgments

Many thanks to George Schut for offering me to opportunity to do my thesis at the company. I would like to thank him for the trust and freedom he has given me to take my own path. Other than that I would like to thank Arie Jonker and Gudo Hartog for their support in the process. I would like to express gratitude to any other person that helped my with my tedious questions. I would like to also thank Bradley Spronk for his superb simulation and his support and effort to help me understanding the workings of it.

I would like thank Steven Hoekstra for facilitating my collaboration with Schut Geometrical Metrology and giving me all the necessary space to execute this research the way I deemed good.

For this thesis generative AI is used. ChatGPT 4o is mostly used and sporadically ChatGPT o4-min-high, if more computation was needed. The models were proven instrumental for finding functions for Mathematica, although often its implementations were faulty. Other than that, it is used for checking grammar, suggesting different way of phrasing sentences, formatting in latex and for brainstorming. It was also specifically used for Figure 5 to achieve a singular color bar.

For example, in the first draft of this thesis, merely the contents of each paragraph were written down in lists. Subsequently, ChatGPT made suggestions on how to put these lists into fully written out paragraphs. Although some phrases are typed over from those suggestions, no full paragraphs are copy-pasted. It was also specifically instructed not to come up with new ideas and merely transform the lists into flowing sentences.

Lastly I would like to thank Ceyda Simsek for the top notch latex template.

1 Introduction

Measurement is important. It is vital in the design of household products, like plastic bottles, or high-precision manufacturing of electronic chips, and everything in between. Entire production lines can become useless if one part is produced out of tolerance.

Schut Geometrical Metrology BV facilitates this need. Other than im- and exporting measurement devices, they also produce their own 3D CNC coordinate measuring machine DeMeet. With both video and touch probe functionalities, they manage a resolution of 0.1 µm [1]. They are, however, always seeking for new technologies to get higher precision and/or faster scanning time.

To achieve this, Schut started developing chromatic confocal sensor technology. This technology uses chromatic aberration—the phenomenon where different wavelengths focus at different distances—to determine longitudinal distances. Companies like Precitec use this technology to get down to nanometer resolution [2].

Previous studies have investigated this principle. Most notably, Ang [3] has managed to develop a prototype capable of rapidly scanning entire surfaces. Furthermore, Hillenbrand et al. [4] published a paper describing the chromatic confocal principle. Schut has also done internal unpublished research: Bradley Spronk [5] developed a set-up proposal and put this set-up in his self-made simulation. The measurement sample in that simulation was modeled as a mirror.

Chromatic confocal imaging works by isolating a distance dependent wavelength range. This happens twice: both for the coaxial light illuminating the sample and for the light of the sample going to the camera. If the set-up is configured correctly, both processes impose the same filtering.

The aim of this study is to continue the research on the principle. Initially, due to limitations of the simulations—both in computing time and capabilities—a simplified version is used. This version is an adaptation of Hillenbrand's design [4] (see Figure 3 in the theory section). In this adaptation, the coaxial illumination system is removed. Note that the light is filtered twice in the same way, thus removing one of the filters does not change the principle. Note that the illumination system would merely lighten a small spot thus to mimic that, the measurement sample will be a small white dot. Also the aperture is placed in between the measurement sample and the first lens. See Figure 1 for a schematic of the simplified version.

The prototype has many configurable settings: the type of lens, the distances between the lenses, the sizes of the diaphragms, etc. This leads to the first research question:

- RQ1: *"Which configuration maximizes measurement accuracy for a chromatic confocal set-up?"*.

To find an answer to this question, a simulation will be used. This simulation is developed by Bradley Spronk. The focus of this thesis will be the diameter of the entrance aperture (element 2 in Figure 1) and the diameter of the pinhole (element 4 in Figure 1). These two elements will be called "aperture" and "pinhole", respectively, throughout this thesis. For these two diameters, a grid search will be executed and the ideal combination will be sought. For the other parameters, theoretical arguments will be made. Section 4.1 will quantify what constitutes "ideal".

Hecht [6] writes, "The surface of an object that is either self-luminous or externally illuminated behaves as if it consisted of a very large number of radiating point sources." Therefore, the measurement sample should be modeled with a number of point sources. To save computation time, the grid search will be first executed with a single point source.

To be able to verify the simulation, a physical set-up will be made. A physical set-up cannot have a point source. Therefore, the second research question is:

- RQ2: *"What influence does the measurement sample diameter have on the measurement accuracy?"*

To find an answer to this question, the measurement sample is modeled with multiple point sources. Given that the simulation is in 2D, a line of point sources—like the ones at element 1 in Figure 1—will represent a dot. The length of the interval in which these point sources lie, represents the sample diameter. Then, this length will be iteratively increased and the results will be analyzed.

1.1 Thesis Outline

Firstly, the necessary theory will be given. This includes a brief introduction to geometrical optics, lens theory, and the principle behind chromatic confocal imaging. After that, the core of this thesis will be presented: the simulation. All its functionalities will be briefly touched upon, incorporated with the set-up that will be used.

Then, the theoretical foundations for the model parameters—excluding the pinhole and aperture radii—will be discussed first. Subsequently, the experimental method used to determine the pinhole and aperture radii will be described.

After that, the approach for the second research question will be given: The width, i.e. the separation of the point sources, will be iteratively increased until the color-distance relation is lost.

Finally, the results of experiments will be presented, followed by a discussion of the limitations and future improvements of the approach, the set-up, and the simulation. The results will be interpreted, a conclusion will be given and a plan for future research will be proposed.

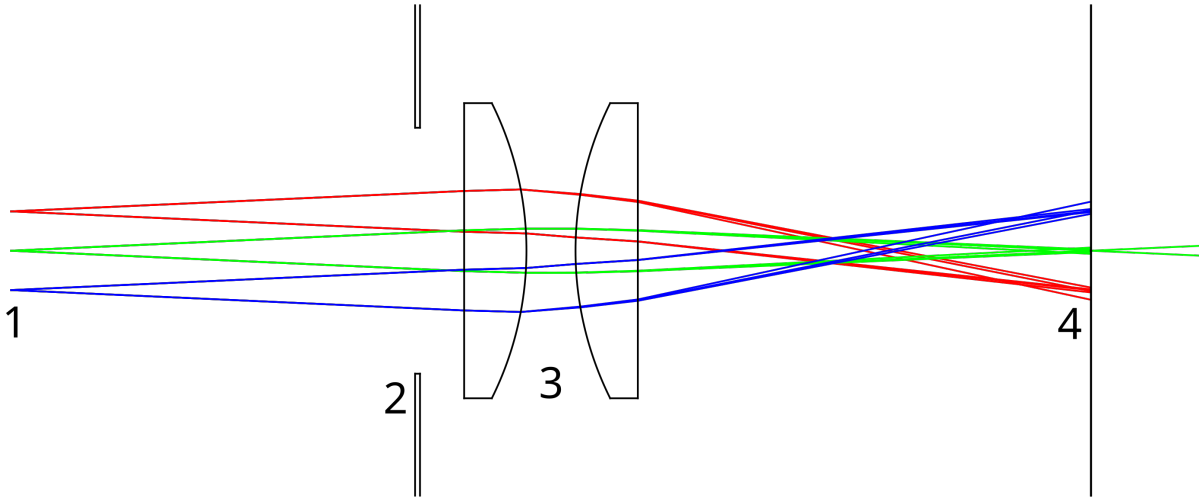

Figure 1: Example set-up for the simulation. At [1], point sources can be placed to model a measurement sample. For simplification, only three points sources are shown with different colors to distinguish them. Also, only two light ray directions per source are displayed and each ray has merely three wavelengths. At [2], an aperture can be placed with variable diameter to block light rays. The lenses at [3] are plano-convex lenses that introduce chromatic aberrations. In this example, only the light ray with a wavelength of 587.5 nm (the design wavelength of the lenses) is transmitted by the pinhole ([4]) while the other rays with wavelengths of 187.5 nm and 987.5 nm are blocked. For this example the diameter of the pinhole is 0.01 mm. The second pair of lenses are omitted for simplicity.

2 Theory

This section introduces the theoretical background necessary to understand the operation of the chromatic confocal imaging principle. It will touch upon geometrical optics, lens theory, aberrations, and the chromatic confocal principle, using primarily Hecht's *Optics* [6].

2.1 Geometrical Optics

Any object can be seen as an infinite number of point sources that radiate spherically outward. Such a point source can then be modeled by rays that are perpendicular to the wave fronts of the spherically outgoing wave. These rays follow the conventional rules for reflections and Snell's law for refraction. This ray-based model is known as geometrical optics and becomes valid when the dimensions of the optical components are much larger than the wavelength of light.

Geometrical optics allows us to treat light as traveling along rays that bend only at boundaries between materials with different refractive indices. However, when the features or apertures become comparable to the wavelength, diffraction effects become significant and this model breaks down. In this thesis, reflections and diffraction are ignored, although the validity of this assumption will be addressed in the discussion.

2.2 Thin Lens Approximation

The purpose of a lens is to focus as much light as possible coming from the point of an object onto its conjugate point in the image. To simplify the calculations for this process, the thin lens approximation is used. In this model, with a lens consisting of two spherical surfaces with radii r_1 and r_2, the space between the two surfaces is treated as negligible ($d_l \to 0$). The surrounding medium is assumed to be air with refractive index $n = 1$, and the paraxial approximation is used, allowing trigonometric functions to be approximated with the first order term in the Taylor series.

The focal length f is the distance from the lens' vertex to the image formed when the object is placed at infinity. This focal length, the image distance s_i , and object distance s_o are related by the thin lens equation:

$$\frac{1}{f} = \frac{1}{s_i} + \frac{1}{s_o}. \tag{1}$$

See diagram for a visualization.

Also, the focal length can be calculated using the Lensmakers' equation:

$$\frac{1}{f} = (n_l - 1)\left(\frac{1}{r_1} - \frac{1}{r_2}\right) \tag{2}$$

where n_l is the index of refraction of the lens. This index turns out to depend on the wavelength of the light that gets diffracted. It is exactly this concept that will be exploited to measure distances with the chromatic confocal imaging technique.

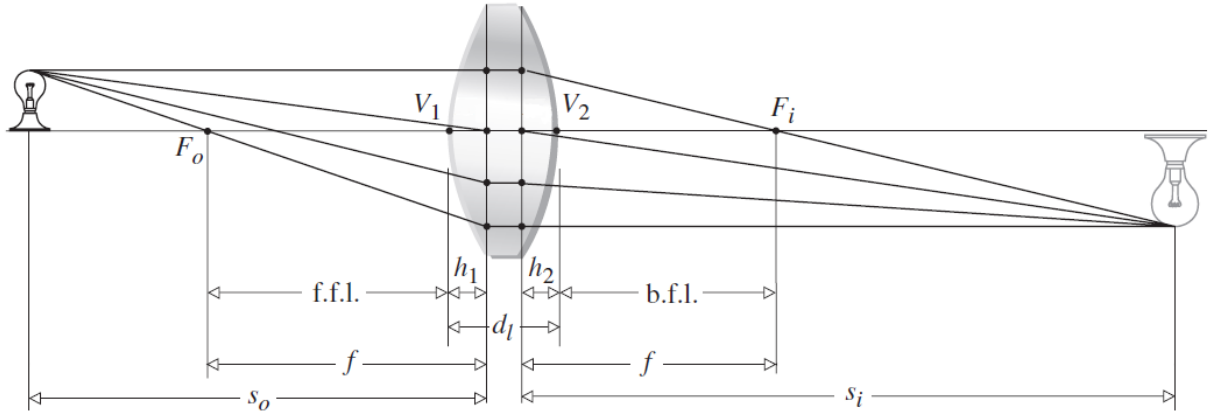

Figure 2: Basic quantities of a thick lens. V_1 and V_2 are the vertices of the lenses, F_o and F_i are the focal points of the object and the image, respectively. See the text for the explanations of the other variables. Adapted from [6].

2.3 Out Of Focus Light

Not only focused light, but also non-focused light will hit the sensor—unless you specifically prevent it. When the light from a point on the object hits the sensor out-of-focus, it will project a blur onto the sensor. The diameter of the blur spot is called the circle of confusion. The distance over which the blur spot stays within the circle of confusion is called the depth of field (DOF).

2.4 Thick Lens Approximation: Cardinal Planes

When the thickness of a lens is non-negligible, the thin lens approximation no longer holds. In that case, the thick lens approximation needs to be used. This includes the concept of the principal planes, with which the fundamental quantities (f, s_i, s_o) get shifted (see Figure 2).

The distance of these principal planes with respect to the center of the lens is given by:

$$\begin{aligned} h_1 &= \frac{f(n_l - 1)d_l}{r_2 n_l} \\ h_2 &= \frac{f(n_l - 1)d_l}{r_1 n_l} \end{aligned} \tag{3}$$

The Lensmakers' Equation gets additional terms:

$$\frac{1}{f} = (n_l - 1)\left[\frac{1}{R_1} - \frac{1}{R_2} + \frac{(n_l - 1)d_l}{n_l r_1 r_2}\right] \tag{4}$$

but equation 1 remains unaltered.

With this introduction, the focal length cannot physically be measured anymore because it is defined with respect to the (abstract) principal plane. To accommodate for this, two new variables are introduced: the front focal length (f.f.l.) and the back focal length (b.f.l.). These are the distances between

the vertex of the lens and the focal point at the back or front side, respectively.

Plano-Convex Lenses
A type of lens that will turn out to be particularly instrumental is the plano-convex lens. It has one flat surface ($r_1 \to \infty$) and one curved surface. The flat side is usually considered the back side and the curved side is considered the front side. This causes the front principal plane to coincide with the vertex and thus the front focal length is the same as the focal length. However, the back focal plane is not equal to zero, thus the back focal length is an important property of a plano-convex lens. The Lensmakers' equation simplifies to

$$\frac{1}{f} = \frac{n_l - 1}{r_2} \tag{5}$$

2.5 Aberrations

Aberrations are deviations from the ideal prediction of the paraxial approximation. They are categorized into two groups: monochromatic aberrations, which affect rays of a single wavelength, and chromatic aberrations, which come from the wavelength-dependent nature of refraction.

2.5.1 Monochromatic Aberrations

There are in total 5 primary monochromatic aberrations: spherical aberration, coma, anti-stigmatism, field curvature and distortion. However, only spherical aberration causes deviation on the optical axis itself. Because for this project mainly the points on the optical axis are considered, only spherical aberration will be considered.

Spherical Aberrations
Spherical aberration is the phenomenon where light rays of greater angles in incidence deviate from the paraxial approximation. Therefore, for plano-convex or biconvex lenses, they focus closer to the lens [1].

2.5.2 Chromatic Aberrations

Low wavelength waves refract more than high wavelength waves because they have a different index of refraction[2]. Therefore, the focus point of low wavelength light is closer to the lens than the focus point of high wavelength light. This causes chromatic aberration. Chromatic aberration is also called dispersion. The more severe the chromatic aberration, the higher the dispersion.

A good measure for the severity of the chromatic aberration is given by Abbe number:

$$V_d \equiv \frac{n_d - 1}{n_F - n_C}, \tag{6}$$

[1] See Appendix A for an example.
[2] For most materials. Validated experimentally with simulation

where n_d is the refractive index at 587.6 nm, and n_F and n_C are at 486.1 nm and 656.3 nm, respectively (The Fraunhofer spectral lines). A small Abbe number gives a high dispersion and vice versa.

An overview of the Abbe numbers of different lens substrates is given by Abbe's diagram, which can be found on schott.com [7].

2.6 Chromatic Confocal Imaging

Hillenbrand et al. [4] made an excellent paper on the topic. The theory presented in this section will be mostly drawn from that paper.

Chromatic Confocal Imaging is a method that uses chromatic aberration to measure distances. Due to this chromatic aberration, different wavelengths focus at different points. A white measurement sample will focus at different positions. Moving the measurement sample along the optical axis will also move these focus points. By filtering out the out-of-focus light, a distance-dependent spectrum around the in-focus wavelength will be isolated. By retrieving the in-focus wavelength, the distance can be traced back.

Given the correct conditions, a pinhole will attenuate out-of-focus light. To get a better understanding of what light goes through a pinhole, one can note that a pixel of the same size at the same location will capture the same light.

Consider a situation where a white point source is focused onto a pinhole and that the pinhole is placed where the design wavelength light is perfectly focused. Because this light is perfectly focused here, no light of the point source will be blocked. The out of focus light will, however, project a blurred spot onto the plane of the pinhole. If the pinhole is smaller than the size of this blurred spot, only a fraction of this blurred spot will go through. The further away the wavelength is from the design wavelength, the bigger the blur and thus the more light that gets filtered out.

However, when the object source gets bigger, the ratio in image size of the in focus light and the out of focus will get smaller because the aberration only causes a blur on the edges of the image. Therefore, it is expected that the pinhole will filter less effectively for bigger sources.

See Figure 3 for the configuration developed by Hillenbrand et al. In this set-up, an illumination system enlightens a pinhole array. These pinholes then form so called "quasi-point sources". The light from these quasi-point sources then are imaged onto the measurement sample using a hyperchromatic lens—a lens that maximizes chromatic dispersion, instead of minimizing.

Because of the symmetry of the set-up, the quasi-point source will project exactly the same pattern of light onto the measurement sample as the measurement sample projects onto the pinhole, except for that the original spectrum of the quasi-point source on the pinhole array is the spectrum of the illumination system and the original spectrum of the measurement sample depends on how it is illuminated. As described before, the pinhole will filter the out-of-focus light. The out-of-focus wavelengths will now be attenuated even more because the out-focus wavelengths will already blurred on the measurement sample and thus had less intensity (per area).

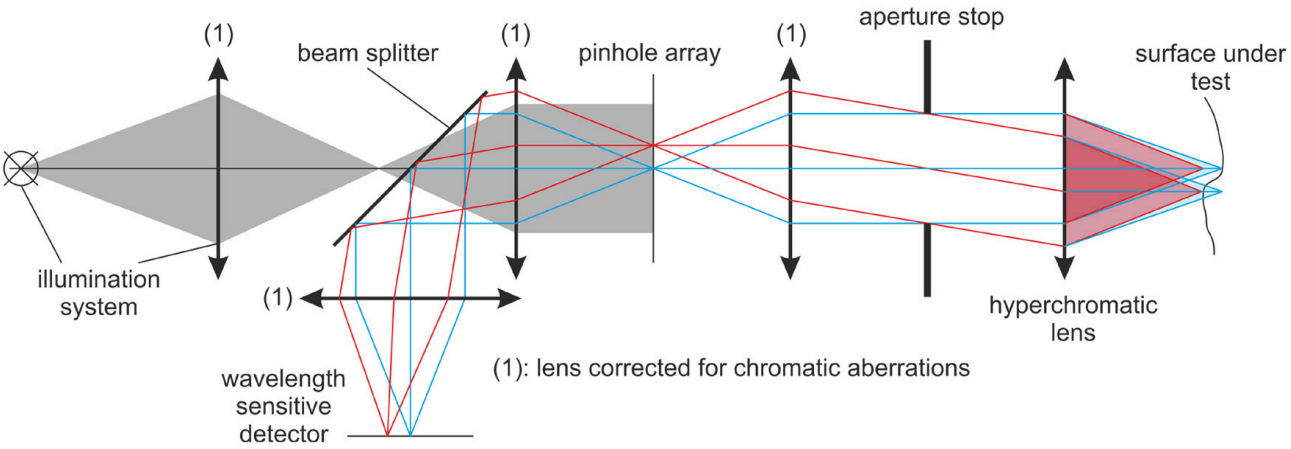

Figure 3: Schematic of the chromatic confocal imaging set-up developed by Hillenbrand et al. A light source shines through a pinhole array, causing quasi-point sources. These are focused onto the measurement sample using a hyperchromatic lens, which introduces chromatic aberration such that different wavelengths focus at different distances. The scattered light from the measurement sample travels back through the same optical path and hits the pinhole array again, causing a second, identical filtering. This filtered light is then focused onto a wavelength-sensitive detector. By analyzing the detected wavelength, the distance to each point on the sample can be determined. [4]

The pinhole array—which has different distance dependent colors for each pinhole—will then be imaged onto a wavelength sensitive detector. Upon analyzing the read-out of the detector the distance is determined for multiple points on the measurement sample.

3 Simulation

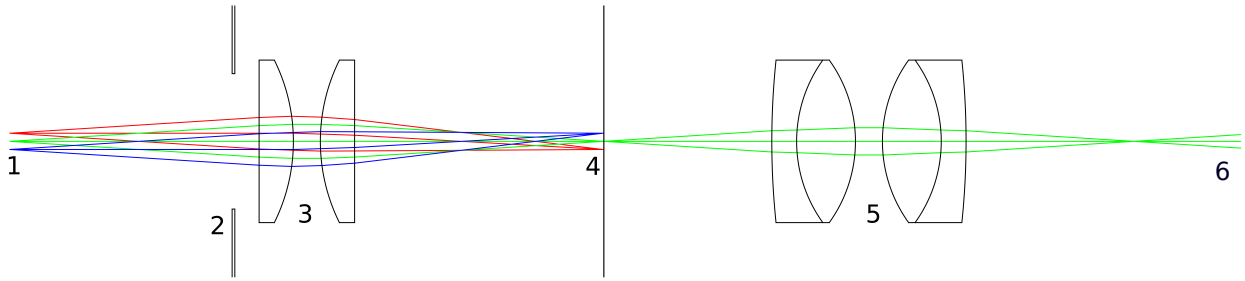

Figure 4: The set-up used for the simulations.

This thesis will make simplifications on the set-up as presented by Figure 3. See Figure 4 for this simplification. Merely one pinhole will be used. Two simple non-achromatic lenses will be used instead of the hyperchromatic lens and the lens corrected for chromatic aberrations. The aperture will be placed before the first lens.

Only the filtering from the measurement sample to the detector will be tested. Therefore, the measurement sample will be illuminated with white light from the sides, instead of coaxial light that has already gone through the pinhole. The coaxial light would have illuminated a small spot on the measurement sample. To still have this effect, the measurement sample will be a small white dot.

For the simulation, further simplifications/approximations will be made. The measurement sample will be modeled with a finite number of point sources. Each point source will emit rays in a number of equally spaced directions. To save computation time, only the rays that end up hitting the lens will be computed. In each direction, rays with different wavelengths are emitted. These wavelengths are uniformly spaced across the visible spectrum (from 380 nm to 750 nm), where each ray has the same wavelength intensity.

These rays will follow the rules of Geometrical Optics where reflections within the lenses are ignored but reflection on the inner edges of the pinhole and aperture are taken into account. For the lenses, the substrate is specified. Every substrate has its own index of refraction as a function of wavelength. The rays that hit the detector (at element 6), can be retrieved and are used to acquire the spectrum.

3.1 Configuration Settings

1: Measurement Sample

- `sourceLocation` Horizontal offset of the source.
- `numberOfSources` The amount of points source that are used in the simulation.
- `lambda` The range of wavelengths for each ray.
- `numberOfColors` The number of wavelengths per ray.
- `rangeAngle` The total angular range (in radians) over which rays are emitted from each point source. The rays are evenly spaced within this range.

- `numberOfRays` The number of rays per points source. Note that in this terminology each ray still consists of multiple wavelengths
- `z` The distance between the source and the flat side of the first lens.
- `a + d` The distance between the vertices of the two curved surfaces (two variables to allow for a filter or aperture in the middle)

2: Entrance Aperture

- `diaphragmDistance` The distance between the aperture and the first lens.
- `sizeAperture` The radius of the opening of the aperture.

3: Plano Convex Lenses

- `substrate` The material of which the lens is made
- `diameter` The diameter of the lens
- `thicknessLens` The thickness of the lens from the left vertex to the right vertex.
- `r1` The radius of the curvature of the curved side of the lens.

4: Pinhole

- `sizeHole` The radius of the opening of the pinhole.
- `b` The distance between the flat side of the second lens and the pinhole

5: Re-Focusing Lenses
Not relevant to the current scope of this thesis, but included to control how the light is focused on the detector.
6: Wavelength sensitive detector
Could be either or spectrograph or an RGB camera. How the wavelength spectrum will be obtained is not the scope of this thesis.

3.2 Experiment Settings

The simulation can be executed multiple times whilst iterating over a certain parameter. The found spectra for each configuration can then be visualized in a heat map. The settings for such an experiment are stated below.

- `iterator` The parameter to iterate over. It can be any of the parameters in section 3.1.
- `numberMeasurements` The number of iterations.
- `begin` The initial value of the iterator
- `end` The value of the iterator at the end of the experiment

4 Approach

In order to answer the research questions, an approach is needed. Firstly, the outcomes that need to be optimized will be determined. As stated before, for the parameters other than the pinhole and aperture diameter, the values will be motivated with theoretical arguments. Then the hypotheses for the diameters will be given. Subsequently, the experiment with which to find these diameters will be given. Lastly, the experiment to find the source width will be given.

4.1 Quantities to be Optimized

Full Width Half Maximum (FWHM)
Consider a point source, a thick lens (see section 2.4) and the conjugate image point of the point source, as displayed in Figure 2. Consider the situation where s_i is fixed. s_o is small if $n(\lambda)$ is high, s_o is big if $n(\lambda)$ is low because light with a wavelength that has a higher index of refraction refracts more. If $n(\lambda)$ decreases monotonically with increasing λ, there exists a one-to-one mapping between s_o and λ.

In this scenario, λ represented the wavelength in focus and s_o represented the distance between the measurement sample and the lens [3], hereafter called the measurement sample distance. Therefore, there exists a one-to-one mapping between the in focus wavelength and the measurement sample distance.

As stated, the pinhole (element [4] in figure 4), isolates a spectrum around the in-focus wavelength, where the in-focus wavelength is filtered the least and the wavelengths around the in-focus wavelength are filtered less and less. However, any measurement sample will emit its own spectrum. Consider a measurement sample that scatters a spectrum that stays within a hundred percent and fifty percent of the maximum wavelength intensity. This spectrum will then be filtered by the chromatic confocal set-up. This means that any detected wavelength with 50 percent of the biggest detected wavelength intensity could be the in-focus wavelength. It is therefore important that any wavelength that is not in-focus is attenuated as much as possible.

In this analysis, a white measurement sample is modeled—i.e. a source that has a uniform wavelength intensity in the visible light spectrum and no wavelength intensity outside. Figure 4 displays this measurement sample at 1. This measurement sample scatters light that will be captured by the camera at element 6. As stated before, the wavelength range around the in-focus wavelength should be as small as possible. The full width half maximum (FWHM) will be used to quantify the width of this range.

The smaller the FWHM, the more accurately the in-focus wavelength can be determined. And, as stated before, this wavelength can be mapped one-to-one to a measurement distance. Thus the FWHM gives a measure how accurate the distance can be measured.

Intensity (Signal Strength)
The pinhole will—by virtue of its purpose—filter out most of the light that comes from the sample.

[3] Technically, one has to take into account the distance between the vertex and the principle plane, but that does not change the argument

In order to accurately measure the color spectrum, this spectrum needs to be considerably brighter than the naturally occurring noise.

Therefore both the intensity captured by the camera—hereafter just called ”intensity” or ”total intensity” if a distinction needs to be made with wavelength intensity—and the FWHM will denote how accurate the measurement distance can be probed.

4.2 Prototype Assumptions

The set-up has many tunable parameters. The aperture diameter, all the characteristics of the lenses, the distances between the objects in the set-up, the size of the pinhole, and all the settings related to how to capture the light with the camera. This thesis will not focus on how to collect the light but will focus on the former parameters. Of those parameters everything but the pinhole size and the diaphragm size will be assumed. Below the theoretical arguments are given for those assumptions.

Spherical aberration is not desirable because it causes the focus points of an object point of a single wavelength to spread out. Therefore, one point on the image side will be the focus points of multiple wavelengths of the same source and it thus becomes more difficult to filter out a single wavelength (or a small range of wavelengths). Therefore, the parameters of the set-up should be chosen in such a way that spherical aberration is minimized, whilst still taking the objectives laid out in section 4.1 into account.

The easiest imaging system is a single biconvex lens. Previous prototypes of internal research had two plano-convex lenses. Because of time constraints, merely a comparison between the biconvex lens and the two plano-convex lenses was made. As seen in Appendix A, the two lens set-up has less spherical aberration and is therefore chosen. Also note that the orientation is chosen such that the angle that the rays make with the lens is minimized.

Lenses have three important properties: the focal length, the diameter and the substrate. Firstly, the focal length determines how strongly the light bends and is highly correlated with the radius of the curved surface of the lens (see equation 5). The smaller the focal length, the smaller the radius of the curved surface, the higher the angles of the rays and thus the higher the spherical aberration, which is not desirable. Therefore, the focal length should be maximized.

Secondly, it is desirable to have the focus points of different wavelengths as far apart from each other as possible such as to more easily filter out small wavelength ranges. Therefore, the lens should treat different wavelengths as distinct as possible. As laid out in the theory, the Abbe number gives such a measure. Therefore, the lens with the lower Abbe number should be chosen.

Lastly, as much light as possible needs to be collected. Therefore, the biggest diameter, given the other constraints/considerations, should be chosen.

Edmund Optics was chosen as a supplier for the lenses. They offer their plano-convex lenses in Fused Silica, N-BK7, N-SF11 and N-SF5 of which the N-SF lenses have the lowest Abbe number [7, 8]. To be compatible with the already available ring light, the lens needs to have a diameter smaller than 50 mm. Out of the N-SF lenses, the lens with product number #88-747 offered the biggest diameter

and the highest focal length whilst still meeting the diameter requirement. This lens also offers the advantage of having an extended visible light coating, which reduces reflections. See Appendix D for the technical drawing of the lens.

4.3 Hypotheses

Pinhole Diameter
With knowing this theory and with knowing what quantities constitute measurement accuracy, hypotheses can be formulated. The first research question is: *"Which configuration maximizes measurement accuracy for a chromatic confocal set-up?"*. As stated before, this study will only experimentally find the diameters of the aperture and the pinhole.

A smaller pinhole will give a smaller wavelength range but also less intensity. It is therefore hypothesized that a smaller pinhole diameter will increase measurement accuracy but only as long as there is enough light intensity to measure a signal.

Aperture Diameter
A bigger aperture will give more spherical aberration because the rays form bigger angles with the surfaces of the lenses. It is hypothesized that this gives a bigger wavelength range. Therefore, a smaller aperture diameter results in improved measurement accuracy. Similar to the pinhole, a smaller aperture diameter results in less intensity and thus a smaller aperture diameter only gives better measurement accuracy insofar the detector is able to detect the intensity.

Source Width
The second research question is: *"What influence does the measurement sample size have on the measurement accuracy?"*. As stated in the theory section, it is expected that for a point source, the in focus light gets isolated perfectly and that the bigger the source size, the worse the wavelength range thus the worse the measurement accuracy.

4.4 Experiments

Pinhole Diameter and Aperture Diameter
To find the optimal pinhole diameter and aperture diameter a grid search is executed for a range of pinhole diameters and aperture diameters. For each combination of pinhole and aperture diameter, the spectra for a range of measurement sample distances is determined. With a spectrum is understood the spectrum of all the light that hits the detector. For each combination of diameters, these spectra are plotted for each measurement sample distance in a heatmap. See Appendix C for the exact configuration of this experiment.

These heat maps will then be further analyzed by extracting the full intensity and the FWHM of each spectrum [4]. Based on this information, a consideration will be made which configuration optimizes accuracy and light intensity.

[4] Technically not all spectra but only the significant ones.

Measurement Sample Diameter

Then the second research question will be investigated: *"What influence does the measurement sample diameter have on the measurement accuracy?"*. For the ideal configuration found in the previous section, the influence of the sample diameter on the FWHM and intensity will be investigated. As stated before, the measurement sample will be a white dot with a diameter to be investigated. This dot will be modeled with point sources that are placed above each other at element 1 in Figure 4. For this experiment, the source width will be increased with a factor of $\sqrt{10}$ until the FWHM exceeds the visible light spectrum.

5 Results

5.1 Aperture Diameter and Pinhole Diameter

As stated in Section 4.1: Quantities to be Optimized, high accuracy can be obtained by minimizing the FWHM of the light that hits the wavelength sensitive detector (element 6 in Figure 4) whilst keeping enough intensity. Therefore, the FWHM and the intensity will be gathered for different configurations to be able to find the ideal configuration.

Grid Search
Figure 5 shows the results for the first research question. As described in the approach (Section 4), these heat maps show the captured spectra for different measurement sample distances. The wavelength goes from 380 nm to 750 nm; the entire visible light spectrum. The range of the horizontal axis is chosen such that the entire curve fits the range.

This horizontal axis denotes the offset with respect to a zero point. This zero point corresponds to the position where, at the design wavelength and in the absence of aberrations, the measurement sample is imaged onto the pinhole. This can be seen by noting that the peak of the spectrum at offset $= 0$ is around 580 mm, the design wavelength of the lenses. Furthermore, the offset is given from left to right, which means that a positive offset denotes a sample closer to the lenses.

FWHM and Intensity
Figure 6a and Figure 6b show the FWHM and the intensity of the upper row of the grid. These values are obtained by analyzing the spectrum at an offset of 2 mm. Figure 6c and Figure 6d show the FWHM and the intensity of the right column. Also for these plots, the middle spectrum with an offset of 2 mm is used. See Table 10 in Appendix B for the values of these plots.

The FWHM is determined by the range of wavelengths of one spectrum that has more than half of the maximum wavelength intensity. Given the discrete nature of the simulation, the accuracy of this measure is the total wavelength range divided by the number of wavelengths that are used. Also, the FWHM will never exceed the wavelength range of visible light (380 nm to 750 nm in the simulation) because there cannot be more rays that are bigger than half the maximum wavelength intensity.

The light intensity is given in the number of simulated rays. Because most of this study is comparative, the unit is of less significance. For the final prototype, the light intensity will be given as percentage of the light intensity coming from the measurement sample.

5.2 Source Width

The second research question is: *"What influence does the measurement sample diameter have on the measurement accuracy?"*. The influence of the measurement sample is investigated for the found parameters for the first research question. The source width will be increased as described in Section 4.4.

Figure 7 shows the heat maps of this experiment. Figure 8 shows the FWHM and the intensity for the different measurement sample diameters. Note that the error bars are merely an indication of how well the FWHM and the intensity are derived from the spectra but do not reflect the accuracy of the

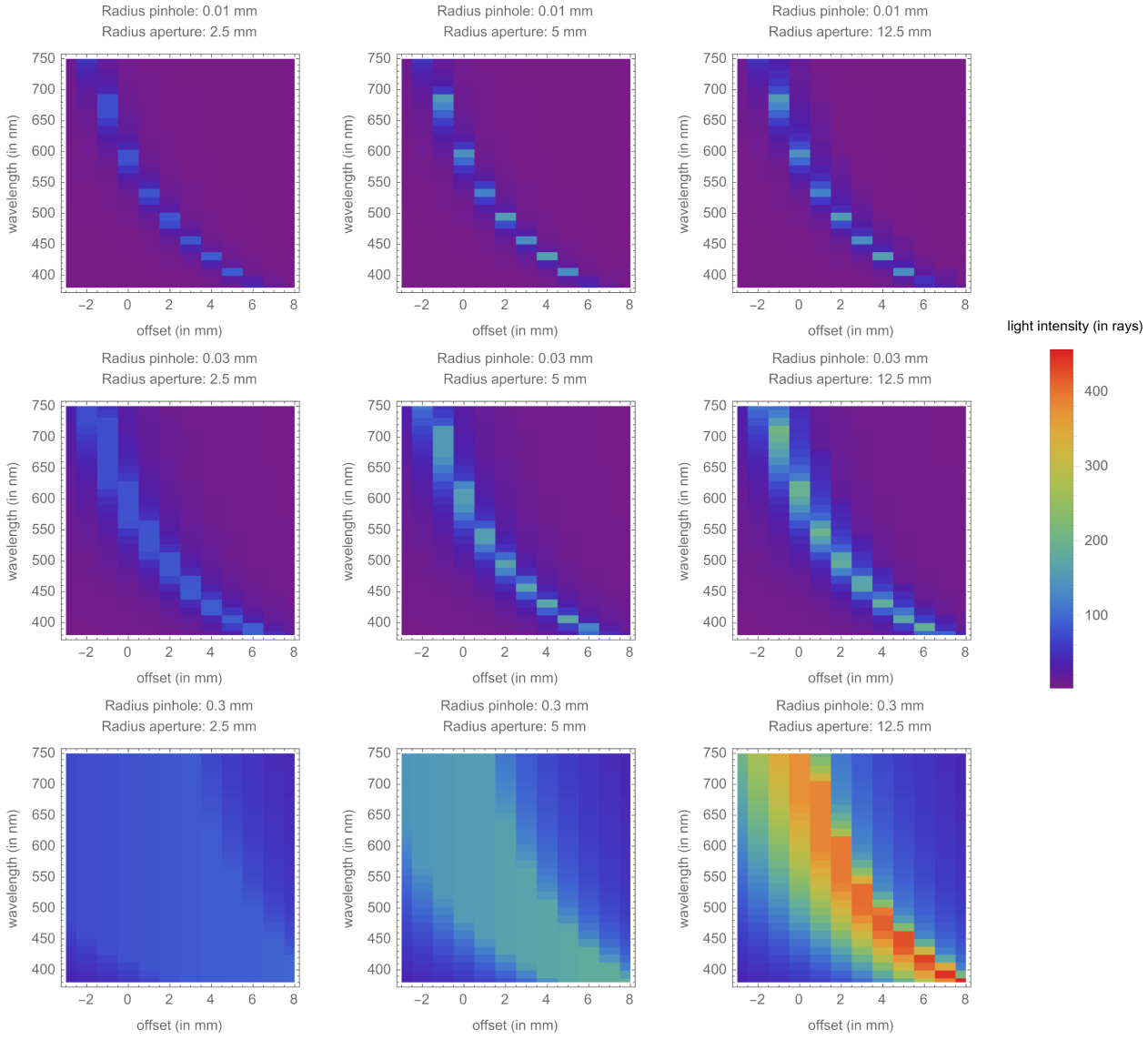

Figure 5: Results of the grid search for pinhole and aperture size. For each heat map, the horizontal axis is the offset of the source with respect to the focal point of the first lens (in mm). The vertical axis is the wavelength of the light (in µm). The color denotes the light intensity. The heat maps increase aperture size to the right and increase in pinhole size going down.

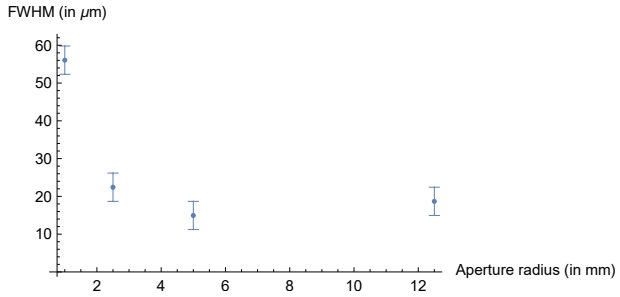

(a) FWHM vs aperture radius with a pinhole radius of 0.01 mm

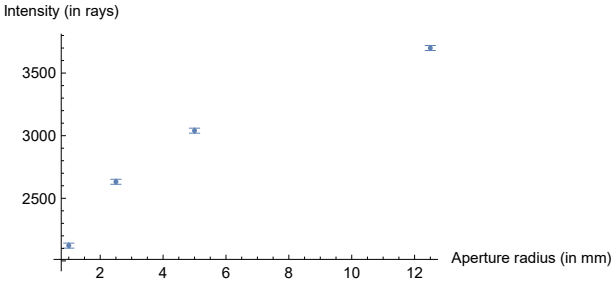

(b) Intensity vs aperture radius with a pinhole radius of 0.01 mm

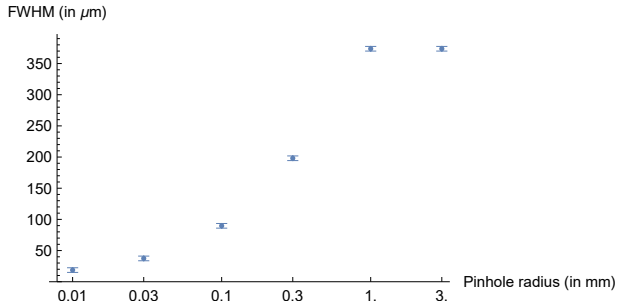

(c) FWHM vs pinhole radius with aperture radius of 12.5 mm

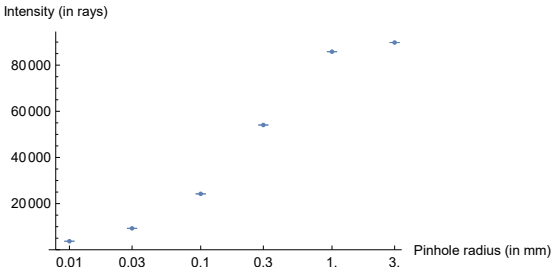

(d) Intensity vs pinhole radius with aperture radius of 12.5 mm

Figure 6: FWHM and intensity vs radii

spectra. To find this, a physical set-up is needed.

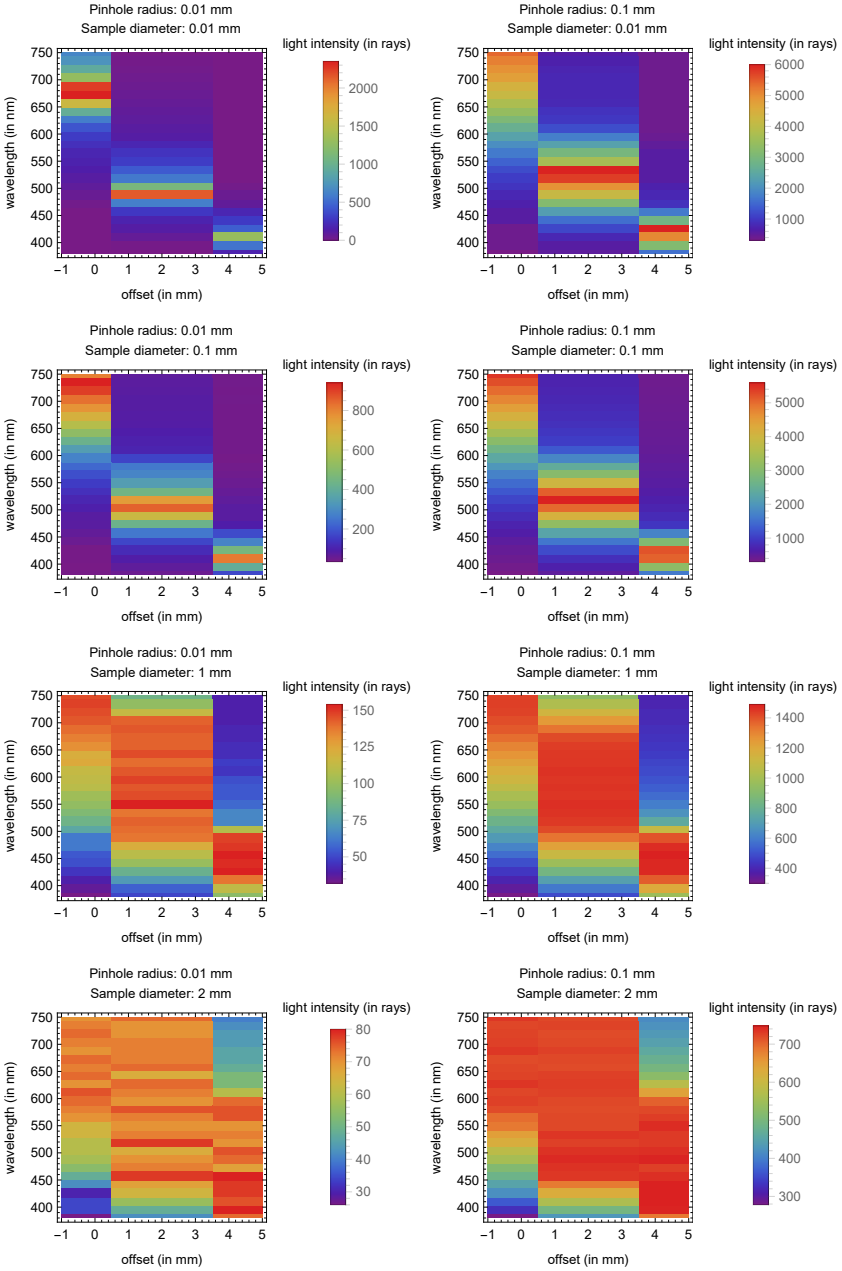

Figure 7: Results of sample sizes iterations. For each heat map, the horizontal axis is the offset of the source with respect to the focal point of the first lens (in mm). The vertical axis is the wavelength of the light (in μm). The color denotes the light intensity in rays, where total light intensity distributed over the sample is held constant. The light intensity per sample area thus decreases with the source width (linearly). The spectrum is only determined for three source locations to save computation time.

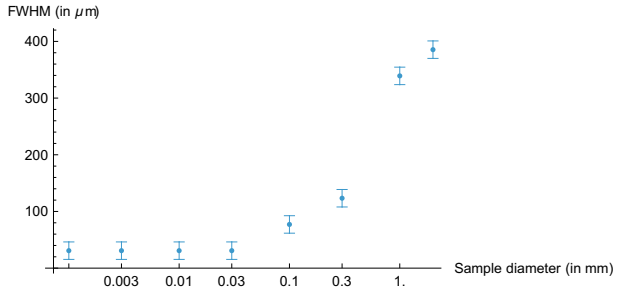

(a) FWHM vs measurement sample diameter with a pinhole radius of 0.01 mm

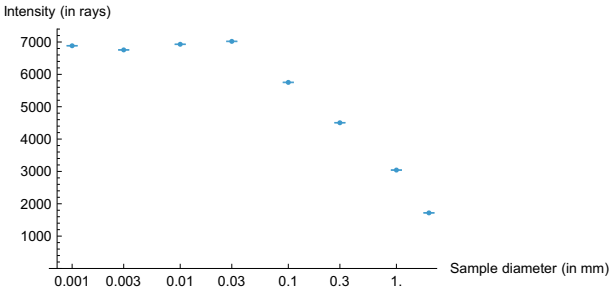

(b) Intensity vs measurement sample with a pinhole radius of 0.01 mm

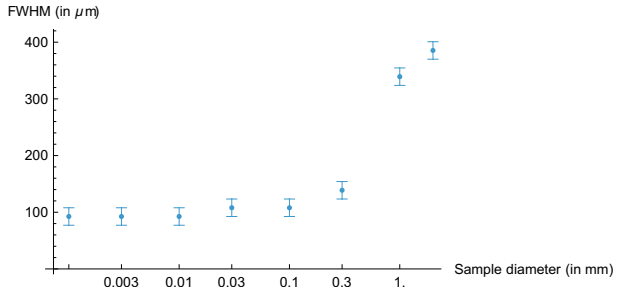

(c) FWHM vs measurement sample diameter with a pinhole radius of 0.1 mm

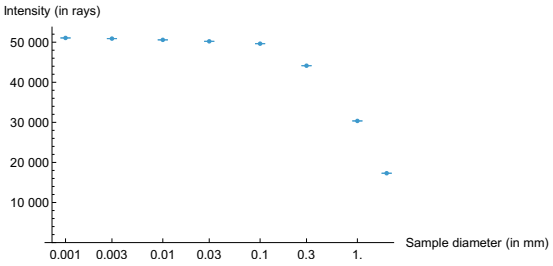

(d) Intensity vs measurement sample diameter with pinhole radius of 0.1 mm

Figure 8: The influence of the measurement sample diameter on the FWHM of the detected spectrum and the total detected intensity.

6 Discussion and Conclusion

6.1 Limitations and Future Suggestions

Set-Up
The full chromatic confocal principle, as explained by Hillenbrand et al. [4], also includes coaxial light. Besides, the configuration of the pinhole size and aperture size are based on a one point source model. It is not clear that these findings will also generalize for both including the coaxial light and/or multiple point sources, i.e. a broader sample size. The simulation should therefore be expanded such that it can handle illumination which allows for the modeling of coaxial lighting. Then, the grid search in Section 5.1 should be repeated with the coaxial light. This will, however, greatly increase simulation time.

Rays hit the pinhole at an angle with respect to the optical axis. The influence of this angle on the filtering process should be investigated. Acquired insights for this concept might influence the choices made in section 4.2: Prototype Assumptions.

Simulation
Also, the simulation is but a rough approximation and it does not account for potentially important factors. It does not account for reflections nor diffraction. Both these factors could influence the results in unexpected ways. Also, the number of rays, the number of sources and the number of wavelengths is in the order of a hundred[5]. It is not clear that these numbers are big enough to simulate the continuous nature of these quantities.

Other than that, the simulation is modeled in 2D. This is partly justified because of the rotational symmetry around the optical axis but more attention should be given to whether an uniform angular emission distribution in 2D also corresponds to a uniform distribution in 3D.

The model does not account for reflections either. Reflection within the lenses and reflections on the edges of the lens tube can have an influence on the results stated in this thesis. Also, future research should model how background light disturbs the signal.

In this thesis, the measurement sample is modeled as a completely diffuse element. However, if the measurement sample has a reflective surface, light will focus at different points. The consequences should be investigated in further research. The measurement sample is also assumed to be a flat surface. The influence of nearby but differently distanced source points should be investigated more.

Also, the measurement sample is assumed to have a uniformly distributed wavelength spectrum. Even though this is taken into account in the interpretation of the results, it should be further investigated how to mitigate problems, such as when the measurement sample fully misses certain wavelengths.

The geometrical optics also fails to capture the physical nature of perfectly focused light. Perfectly focused light forms an Airy disk and the consequences of this phenomena should be investigated further.

For this research the width of the spectrum is quantified by the FWHM. The FWHM could be more accurately acquired by fitting an appropriate distribution through the spectrum instead of merely count-

[5] See appendix C for the exact number of rays used for the different experiments.

ing the number of wavelengths that exceed half the maximum. Also, more research should be done on how to more accurately determine the in-focus wavelength from the spectrum.

Also, during the research, it was found that blocking light rays that go straight from the source to the camera improved the quality of the detected spectra. Instead of a detected spectrum with a long tail, no wavelength intensity was measured outside a certain wavelength range. This phenomenon should be further researched.

Approach
As of the writing of this thesis, the results of a physical prototype are not available yet. Oversights can be made in the production of the model; thus, the results should be verified with a physical set-up.

This thesis only experimented with pinhole and aperture size, but every other parameter of the set-up deserves its own experiment.

For the monochromatic aberrations, only spherical aberration is considered because most of the off-axis light is blocked by the pinhole. However, other monochromatic aberrations might have significant influences on points on the measurement sample around the optical axis and points around the optical axis within the pinhole. These effects must be investigated.

It would also be valuable to develop a mathematical model for the wavelength to distance relationship. This would not only give insight on how to extract the in-focus wavelength from a wavelength range, it would also aid in manipulating this curve to get a bigger measurement range and/or a higher precision.

In this study, the term intensity is used somewhat inconsistently. At the start of the setup, it is introduced as the radiation from a point source emitting equally in all directions. Later, however, it's treated as the signal received by the camera, meaning the total photon count integrated over the detector area and shutter time. This discrepancy isn't too problematic for this research, since only relative comparisons between different setups are made. Still, future work should accommodate for this.

Literature Research
Hillenbrand [4] and Ang [3], have done extensive research on the topic. A more thorough research on these materials would have given better insight into the choices made in section 4.2. Other than that, Sensofar [9] has done commercial research, and studying these materials could have given valuable insights.

Also, more research can be done on what configurations of lenses give the best result. A set-up should be created that actively tries to increase chromatic aberrations whilst keeping spherical aberrations to a minimum. Aspherical lenses—lenses with non-spherical surfaces that reduce spherical aberration—should be researched.

It should also once again be noted that the values given in Figure 6 and 8 are merely for comparison. The accuracy of this value should be determined by a physical set-up. The main purpose of them is to compare set-ups such that an educated guess can be made which configurations should be used for the prototype.

Other than the before mentioned improvements, the following explicit research questions can be in-

vestigated:

- Is spherical aberration truly harmful for getting a useful color-distance relation?
- If yes, what is more viable: reducing the aberration with multiple lenses or with a single aspherical lens?
- What benefits does coaxial lighting give?
- Hillenbrand et al [4] use a telecentric set-up. What are the advantages of this?
- How can the measurement range be influenced?

6.2 Interpretation of the Results

The results show that, even without coaxial lighting but with a single point source, a correlation can be found between the detected spectrum and distance of measurement sample.

Aperture
Figure 6a shows that there is a negative correlation between the FWHM and the aperture diameter. Figure 6b shows that there is a positive correlation between the total intensity received by the detector (element 6 in figure 4) and the aperture diameter. This means that the biggest diameter gives both the best accuracy and the best signal strength.

Figure 6a is based on the upper row of the grid search 5. Given that the heat maps of the rows show similar trends it can be assumed that for all pinholes, the maximum aperture gives the best accuracy. Note that the maximum aperture is 25 mm and which, with the configuration, allows all light from the measurement sample to fall on the lens. It is therefore found that no aperture gives the best results. However, the aperture will still be placed in the set-up to prevent reflection on the inner edges of the lenses.
As expected, a smaller pinhole does seem to reduce FWHM and thus increase measurement accuracy. Also as expected, a smaller pinhole does decrease intensity. It should therefore be researched how much intensity is needed to still observe the spectrum.

Measurement Sample Diameter
Figure 8 shows, as expected, that the measurement accuracy gets worse with increasing measurement sample diameter. The FWHM stays approximately constant as long as the sample is smaller than the pinhole but quickly worsens when the sample gets bigger. Interestingly enough, both pinhole sizes give approximately the same result for a sample of 0.3 mm. Suggesting that the pinhole size ultimately matters less than previously stated. Getting a pinhole size of 0.3 mm will not be easy to obtain thus it is advised to implement the coaxial lighting as done Hillenbrand to be able to measure a distance. However, as seen in Figure 7, a color difference must still be observed by moving the measurement sample. Therefore, implementing the suggested set-up will still proof valuable for verifying the simulation. However, noise is not taken into account thus it could still happen that no color shift will be observed.

The source width seems to still be small enough up to 2 mm. More measurements should be done with bigger source widths and it should be investigated whether reflection, diffraction and/or background

noise is significant enough to blur the color-distance relationship of the 2 mm source width.

Because the grid search is only performed with a single point source, it should be researched whether the results generalize to bigger sample sizes.

An unexpected outcome is that the center wavelength vs distance relationship seems to not be constant with varying source widths. It should be given attention whether the assumptions surrounding the middle wavelength logic are sound and it should, therefore, be researched whether this can be mitigated.

6.3 Conclusion

The research questions can now be answered. The first research question is: *"Which configuration maximizes measurement accuracy for a chromatic confocal set-up?"*. This study has found that the set-up as given by 4 maximizes accuracy, given the assumption made in this research. This set-up has two plano-convex lenses, with Edmund Optics model number #88-747 (see Section 4.2). The aperture inner radius (element 2) is 12.5 mm. Because a smaller pinhole (element 4) causes both higher measurement accuracy but also less signal strength detected by the camera, two prototypes are suggested with two different pinhole radii: 0.01 mm and 0.1 mm. The bigger radius causes a better signal strength but less measurement accuracy and the smaller radius vice versa. Future research with a physical set-up should compare the two prototypes.

To put these numbers in perspective, the intensity can be compared to the total number of rays emitted by the measurement sample (225 000, see Listing 4 in Appendix C). This gives relative intensity of 1.5 % and 10 %, respectively, approximately.

As seen in the grid search (Figure 5), the measurement range is approximately 6 mm. Prototype 1 has a FWHM of 5 % of the visible spectrum thus this would give a measurement accuracy of about 0.3 mm, assuming a linear correlation. By the same logic, prototype 2 has a measurement accuracy of 1.5 mm. See Table 3 for an overview. Once again, these numbers are purely for comparison and should be taken as accurate only to their order of magnitude.

Lens set-up	See Figure 4
Lens model number	Edmund Optics: #88-747
Pinhole radius	0.01 mm
Aperture radius	12.5 mm

Table 1: Prototype 1

Lens set-up	See Figure 4
Lens model number	Edmund Optics: #88-747
Pinhole radius	0.1 mm
Aperture radius	12.5 mm

Table 2: Prototype 2

	FWHM (in μm)	Measurement Accuracy (in mm)	Intensity (in rays)	Intensity (in %)
Prototype 1	19 ± 4	≈ 0.3 mm	≈ 3500	$\approx 1.5\%$
Prototype 2	90 ± 4	≈ 1.5 mm	≈ 25000	$\approx 10\%$

Table 3: Comparison of FWHM and Intensity for both prototypes

The second research question is: *"What influence does the measurement sample diameter have on the measurement accuracy?"*. With a measurement sample smaller than 0.3 mm a distance should be able to be measured but bigger than that causes the FWHM equally large as the visible light spectrum. The set-up could however still be tested to verify the simulation. To get higher accuracies, the coaxial lighting given by Hillenbrand [4] should be investigated.

6.4 Outlook

The prototype as described is already built. It will be tested whether the color change as predicted by the right lower heat map in Figure 7 happens for a measurement sample of 2 mm. This will be done for both suggested pinhole radii. If no color change is observed, the points earlier suggested in this discussion will have to be implemented. The most promising of them is the coaxial illumination system as described by Hillenbrand [4] (see Figure 3).

Another promising improvement is the annulus. This can be relatively easily added to the simulation and the full analyses should be repeated.

When a configuration is found that has FWHM significantly smaller than the visible light range, the spectrum needs to be interpreted. This will be done by an RGB camera. Ang [3] describes how this should go. It will skip the spectrum and directly calibrate RGB with distance.

Bibliography

[1] "Technical specifications." Schut.com. Accessed: Jun. 14, 2025. [Online]. Available https://www.schut.com/Products/DeMeet/index_Specifications.htm.

[2] "Ultra-fast distance measurements of almost all materials: How chromatic confocal sensor technology works." Precitec.com. Accessed: Jun. 26, 2025. [Online] Available: https://www.precitec.com/optical-3d-metrology/technology/chromatic-confocal-sensors/.

[3] K. T. Ang, "High Speed Confocal 3D Profilometer: Design, Development, Experimental Results." Ph.D. thesis, Dept. of Elect. and Comput. Eng., Nat. Univ. of Singapore, Singapore, 2014.

[4] M. Hillenbrand, A. Gewe, and S. Sinzinger, "Parallelized chromatic confocal systems enable efficient spectral information coding," *SPIE Newsroom*, 2013.

[5] B. Spronk. Private comunication, 2025.

[6] E. Hecht, *Optics*. Addison Wesley, 2nd ed., 1987.

[7] SCHOTT AG, "Interactive abbe diagram." https://www.schott.com/en-us/special-selection-tools/interactive-abbe-diagram, 2024. Accessed: 2025-06-06.

[8] M. N. Polyanskiy, "Refractiveindex.info database of optical constants," *Scientific Data*, vol. 11, p. 94, 2024.

[9] Sensofar, "Sensofar papers." [Online], Available: https://www.sensofar.com/metrology/technology/sensofar-papers/, 2025. Accessed: 2025-06-17.

Appendices

A Comparing Lenses

As seen in Figure 9, the two lens set-up has less spherical aberration. Equation 1 (which is equivalent for thick lenses) is used for the calculation of the source to lens distance. Note that error bars are just for illustration and that the values are given with too many significant digits.

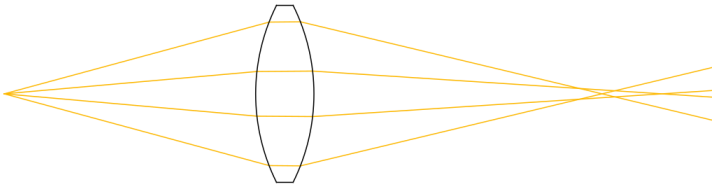

(a) One lens

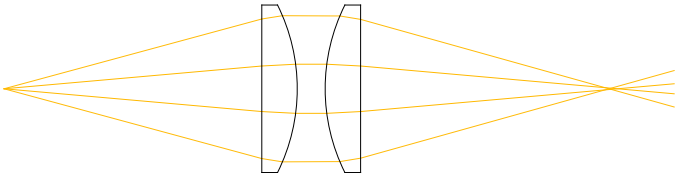

(b) Two lenses

Figure 9: Illustration of spherical aberration for different lens configurations.

B Tables of Plots

See Figure 10 for the tables of the FWHM and intensity plots of Section 5.1.

See Figure 11 for the table of the FWHM and intensity plots of section 5.2.

Aperture radius (in mm)	FWHM (in μm)
1	56. ±4.
2.5	22. ±4.
5	15. ±4.
12.5	19. ±4.

(a) FWHM vs aperture radius with a pinhole radius of 0.01 mm

Aperture radius (in mm)	Intensity (in rays)
1	2122. ±20.
2.5	2632. ±20.
5	3040. ±20.
12.5	3700. ±20.

(b) Intensity vs aperture radius with a pinhole radius of 0.01 mm

Pinhole radius (in mm)	FWHM (in μm)
0.01	19. ±4.
0.03	37. ±4.
0.1	90. ±4.
0.3	198. ±4.
1	374. ±4.
3	374. ±4.

(c) FWHM vs pinhole radius with aperture radius of 12.5 mm

Pinhole radius (in mm)	Intensity (in rays)
0.01	3700. ±20.
0.03	9280. ±20.
0.1	24 228. ±20.
0.3	54 066. ±20.
1	85 832. ±20.
3	89 800. ±20.

(d) Intensity vs pinhole radius with aperture radius of 12.5 mm

Figure 10: FWHM and intensity vs radiuss

C Settings for Experiments

Listing 1: Configuration for the pinhole and aperture grid search (Figure 5)

```
(*Elements: confocal lenses *)
thicknessLens = 6.35;
diameter = 30;
r1 = 33.63;
backFocalLength = 46.17;
substrate = "N-SF5"

(*Distances *)
a = 2.5;
b = 46.17;
d =  2.5;
z = 46.17;
distanceAperture = 5;

(*Simulation*)
numberOfRays = 100;
numberOfColors = 30;
\[Lambda] = {380, 750};
numberOfSources = 1;
sourcewidth = 1;

(* Heatmap settings *)
```

Sample diameter (in mm)	FWHMM (in μm)
0.001	31. ±15.
0.003	31. ±15.
0.01	31. ±15.
0.03	31. ±15.
0.1	77. ±15.
0.3	123. ±15.
1	339. ±15.
2	385. ±15.

(a) FWHM vs measurement sample diameter with a pinhole radius of 0.01 mm

Sample diameter (in mm)	Intensity (in rays)
0.001	6884. ±10.
0.003	6756. ±10.
0.01	6930. ±10.
0.03	7020. ±10.
0.1	5752. ±10.
0.3	4504. ±10.
1	3042. ±10.
2	1718. ±10.

(b) Intensity vs measurement sample with a pinhole radius of 0.01 mm

Sample diameter (in mm)	FWHMM (in μm)
0.001	93. ±15.
0.003	93. ±15.
0.01	93. ±15.
0.03	108. ±15.
0.1	108. ±15.
0.3	139. ±15.
1	339. ±15.
2	385. ±15.

(c) FWHM vs measurement sample diameter with a pinhole radius of 0.1 mm

Sample diameter (in mm)	Intensity (in rays)
0.001	51 062. ±10.
0.003	50 896. ±10.
0.01	50 584. ±10.
0.03	50 218. ±10.
0.1	49 632. ±10.
0.3	44 134. ±10.
1	30 356. ±10.
2	17 306. ±10.

(d) Intensity vs measurement sample diameter with pinhole radius of 0.1 mm

Figure 11: The influence of the measurement sample diameter on the FWHM of the detected spectrum and the total detected intensity.

```
numberMeasurements = 12;
sourceLocation := iterator;
begin = 8;
end = -3;

(* Explored parameters *)
{sizeHole, {0.01, 0.03, 0.1 , 0.3}}, {sizeAperture, {1, 2.5, 5, 12.5}}
```

Listing 2: Configuration for the FWHM and intensity vs aperture radius (Figure 6a and 6b)

```
(*Elements: apertures, will not be used for this simulation because \
these parameters are iterated over*)
sizeHole = 0.01;

(*Elements: confocal lenses *)
thicknessEdge = 2.82;
thicknessLens = 6.35;
diameter = 30;
r1 = 33.63;  (* Radius of curvature of the plano-convex lens *)
backFocalLength = 46.17;
substrate = "N-SF5";

(*Distances, see technical drawing (z=e) *)
a = 2.5;
b = 46.17;
d =  2.5;
z = 46.17;
distanceAperture = 5;

(*Simulation*)
numberOfRays = 1000;
numberOfColors = 100;
\[Lambda] = {380, 750};
numberOfSources = 1;

(* Grid search *)
numberMeasurements = 3;
begin = 3;
end = 1;
sourceLocation := iterator

(*Explored parameters *)
sizeAperture, {1, 2.5, 5, 12.5}
```

Listing 3: Configuration for the FWHM and intensity vs pinhole radius(Figure 6c and 6d)

```
(*Elements*)
sizeHole = 0.01;
```

```
(*Elements: confocal lenses *)
thicknessEdge = 2.82;
thicknessLens = 6.35;
diameter = 30;
r1 = 33.63;  (* Radius of curvature of the plano-convex lens *)
backFocalLength = 46.17;
substrate = "N-SF5";

(*Distances, see technical drawing (z=e) *)
a = 2.5;
b = 46.17;
d =  2.5;
z = 46.17;
distanceAperture = 5;

(*Simulation*)
numberOfRays = 1000;
numberOfColors = 100;
lambda = {380, 750};
numberOfSources = 1;

(* Grid search *)
numberMeasurements = 3;
begin = 3;
end = 1;
sourceLocation := iterator

(*Explored parameters *)
sizeHole, {0.1 , 1, 0.03, 0.3, 3}
```

Listing 4: Configuration for the source width experiment (Figure 7)

```
(*Elements: apertures*)
sizeAperture = 12.5;
substrate = "N-SF5"

(*Elements: confocal lenses *)
thicknessLens = 6.35;
diameter = 30;
r1 = 33.63;
backFocalLength = 46.17;

(*Distances*)
a = 2.5;
b = 46.17;
d =  2.5;
z = 46.17;
```

```
distanceAperture = 5;

(*Simulation*)
numberOfRays = 90;
numberOfColors = 25;
numberOfSources = 100;
sourcewidth = 1;
\[Lambda] = {380, 750};
sourceLocation = 0;
offset = 0;

(* Heatmap settings *)
numberMeasurements = 3;
begin = 5;
end = -1;

(* Experiment settings *)
sourceLocation := iterator;

(* Explored parameters *)
{sizeHole, {0.1, 0.01}}
,
{sourcewidth, {2, 1, 0.3, 0.1, 0.03, 0.01, 0.003, 0.001} }
```

D Technical Drawing Lens

See Figure 12 for the technical drawing of the plano-convex lens used in the set-up.

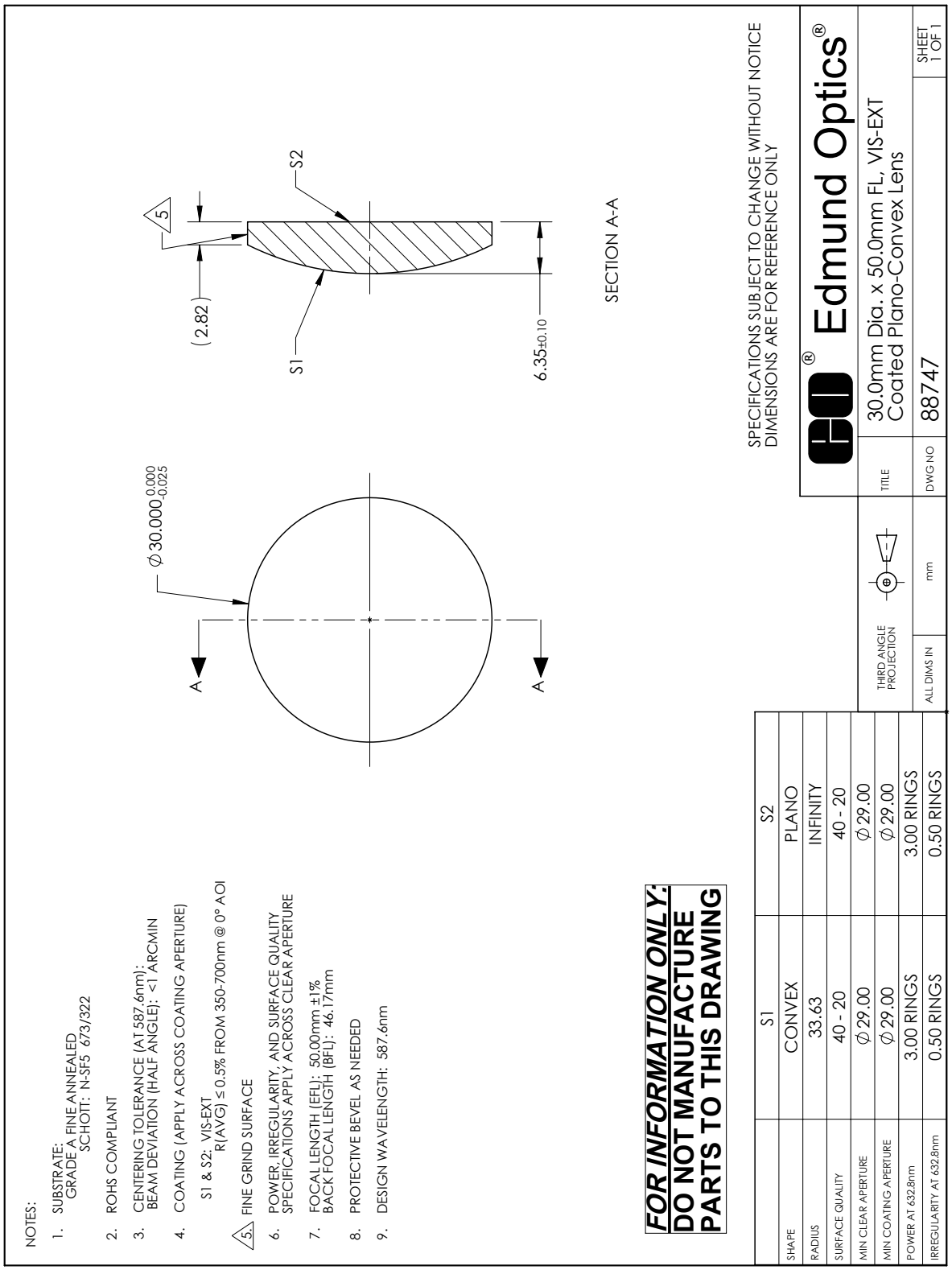

Figure 12: Technical drawing of the plano-convex lens used in the set-up (element 3 in Figure 4).